

# Lidar and sun photometer measurements of aerosol optical properties over Taipei

Wei-Nai Chen<sup>1</sup>, Yei-Wei Chen<sup>1,2</sup>, Shih Yu Chang<sup>1</sup>, Charles C.-K. Chou<sup>1</sup>, Jen-Ping Chen<sup>2</sup>

<sup>1</sup>Research Center for Environmental Changes, Academia Sinica

<sup>2</sup>Department of Atmospheric Science, National Taiwan University

## Abstract

Tropospheric aerosols have been observed for the spring and winter periods from February 2004 to January 2006 with a lidar and a CIMEL sun photometer. Variations of aerosol vertical profile and column optical thickness derived from the lidar and the sun photometer measurements are presented. The simultaneous measurements of these instruments also allowed us to estimate the extinction-to-backscatter ratio (so called lidar ratio), which ranged from 20 to 80. The correlation between angstrom exponents derived from sun photometer and lidar ratio for the columnar mean aerosols were discussed. Seasonal (Oct-Jan and Feb-May) dependence is found between aerosol angstrom exponent and lidar ratio. In Feb-Apr, fraction of aerosol in the free atmosphere is higher than other months. With depolarization measurement we notice the correlations between angstrom exponent and lidar ratio are different in Asian dust dominated episodes and non-dusty episodes.

## 1. Introduction

Aerosol optical depth (AOD) indicates the column-integrated burden in the atmosphere and is a main parameter of the aerosols that significantly impacts the climate. Lidar is powerful techniques for active remote sensing of the vertical profile of troposphere with high temporal and spatial resolution. The effects of aerosols represent one of the largest uncertainties in predicted climate change (Haywood and Boucher, 2000). In this paper, we present the optical characteristics of aerosols over Taipei as they are determined by lidar and sun photometer. We briefly describe the instrumentation we used for this study. The optical characteristics determined from these measurements are discussed and compared with the ones from studies that correspond to regions with Asian dust burning episodes.

The intensive optical properties (independent on concentration) of aerosol such as Angstrom exponent and extinction-to-backscatter ratio (or so called lidar ratio) are complicated functions of aerosol size distribution, composition, and shape. Angstrom exponent  $\alpha$  is a good indicator of the size of particles. Higher values ( $\alpha > 2$ ) are typically observed for accumulation mode particles and lower values ( $\alpha$  near 0) have been observed for coarse mode particles, Saharan dusts and Asian dusts (Eck et al., 1999; Sakai et al., 2002). The value of lidar ratio varies with characteristic of aerosols. Lidar ratio was usually treated as "characteristics" of particles and had been widely applied to identify type of particle such anthropogenic aerosol, dust particle, and cloud. Lidar or in-situ measurements and computer simulations show

lidar ratio for sea salt, Asian dust, Saharan dust, biomass burning, and urban aerosol are 20-30 sr, 40-60 sr, 30-40 sr, 45-65 sr, and 20-80 sr, respectively (Ansmann et al., 1992a; Takamura et al., 1994; Anderson et al., 2000; Liu et al., 2002).

## 2. Instruments and Method

RCEC/ASNTU Lidar is a dual-wavelength Raman and Depolarization Lidar system installed at weather observatory of Department of Atmospheric Science of National Taiwan University. The lidar system employs the second and third harmonics of Nd-YAG laser at 532 nm and 355 nm. The lidar equation can be expressed as

$$P_{\lambda}(z) = P_{\lambda} \frac{A}{z^2} \beta_{\lambda}(z) T_{\lambda_i}(z_0, z) T_{\lambda}(z_0, z)$$

where  $\lambda_L$  is the laser wavelength,  $P_{\lambda_L}$  is the laser power,  $P_{\lambda}(z)$  is the measured lidar signal at wavelength  $\lambda$  returned from altitude  $z$ ,  $A$  is the system calibration factor,  $\beta_{\lambda}(z)$  is the volume Rayleigh/Mie or Raman backscattering coefficient of the scattering media at  $\lambda$ , and  $T_{\lambda}(z_0, z)$  are the atmospheric transmission at  $\lambda$  between lidar at altitude  $z_0$  and  $z$ .

$$T_{\lambda}(z_0, z) = e^{-\int_{z_0}^z (\sigma_{m,\lambda}(z') + \sigma_{a,\lambda}(z')) dz'}$$

where  $\sigma_{m,\lambda}(z)$  and  $\sigma_{a,\lambda}(z)$  are volume extinction coefficients of air molecule and aerosol at  $\lambda$ . Aerosol backscattering ratio  $R$  is define as

$$R_{\lambda}(z) = 1 + \frac{\beta_a(\lambda, z)}{\beta_m(\lambda, z)}$$

where  $\beta_{a,\lambda}(z)$  and  $\beta_{m,\lambda}(z)$  are volume backscattering coefficient of aerosol and air molecule at  $\lambda$ , respectively. To derive analytical solution for the lidar equation, it has been commonly assumed these parameters are related in the form of the aerosol extinction-to-backscatter ratio or so called lidar ratio  $S_\lambda$ .

$$S_\lambda = \frac{\sigma_\lambda}{\beta_\lambda}$$

Solving the lidar equation requires to know how lidar ratio varies along the light path (Klett, 1981; Fernald, 1984). Since Raman signal is not available at daytime owing to strong sunlight, in this study, we try to apply column aerosol optical thicknesses measured by sun photometer as a constraint of signal inversion to derive "column" lidar ratio to improve the accuracy of lidar vertical profiles.

The aerosol optical depth (AOD) was also retrieved from the radiances measured by the Cimel Electronique CE318-1 automatic sun-tracking sun photometer installed at lidar site. This instrument had seven filters centered at 340, 380, 440, 500, 675, 870, and 1020 nm. The spectral dependence (Angstrom exponent) of AOD is important for modeling the radiative effects of aerosols on the Earth/atmosphere system and is related to the aerosol size distribution which is defined as:

$$\alpha = -\frac{d \ln AOD(\lambda)}{d \ln \lambda}$$

### 3. Results and conclusion

During Feb. 2004 to Jan. 2006, there are 103 coincided lidar and sun photometer measurements. Figure 1 shows the monthly average values of aerosol optical thickness for coincided lidar and sun photometer measurements (dashed line) and whole set (solid line) of sun photometer during Feb. 2004 to Jan. 2006.

Figure 2 shows two lidar profiles measured at 2004/2/18 10:09 LT (local time) and 2004/11/10 11:53 LT to demonstrate aerosol vertical profiles and lidar ratios. Owing to signal reducing problem caused by overlap between laser beam and field of view of telescope, we assume aerosols were well mixed at height below 400 m. For cases that mixing height lower than 400 m are removed from data list. The Monthly averaged vertical distributions of aerosol backscattering ratios measured by lidar at winters (Oct-Jan) and springs (Feb-May) are shown in Figure 3. Monthly average values of AOD, Angstrom exponent, and lidar ratio derived from combined sunphotometer and lidar measurements are shown in Table 1. Fractions of AOD contributed by aerosol above 1.5 km are also shown in Table 1. The result shows more than 30% of AOD at February, March, and April are contributed by aerosols distributed at altitude higher than 1.5 km.

Figure 4 shows the scatter diagram of CIMEL angstrom exponent versus lidar ratio for the winter and

the spring periods. Seasonal (Oct-Jan and Feb-May) dependence is found between aerosol angstrom exponent and lidar ratio. In Feb-Apr, fraction of aerosol in the free atmosphere is higher than other months. With depolarization measurement we notice the correlations between angstrom exponent and lidar ratio are different in Asian dust dominated episodes and non-dusty episodes. Figure 5 shows scatter diagram of angstrom exponent versus lidar ratio same as Figure 4 but categorized by AOD fractions of Asian dust. It could be noticed that anthropogenic aerosols (spherically shaped) and Asian dusts (total depolarization ratio higher than 8%) exhibit different correlations that may be caused by irregular shape of dusts (Mishchenko and Sassen, 1998).

### References

- Anderson, T. L., Masonis, S. J., Covert, D. S., Charlson, R. J., Rood, M. J., 2000. In situ measurement of the aerosol extinction-to-backscatter ratio at a polluted continental site. *Journal of Geophysical Research* 105, 26907–26916.
- Ansmann, A., Riebesell, M., Wandinger, U., Weitkamp, C., Voss, E., Lahmann, W., Michaelis, W., 1992a. Combined raman elastic-backscatter LIDAR for vertical profiling of moisture, aerosol extinction, backscatter, and LIDAR ratio. *Applied Physics B: Lasers and Optics* 55, 18–28.
- Eck, T. F., Holben, B. N., Reid, J. S., Dubovik, O., Smirnov, A., O'Neill, N. T., Slutsker, I., Kinne, S., 1999. Wavelength dependence of the optical depth of biomass burning, urban, and desert dust aerosols. *Journal of Geophysical Research* 104, 31333–31350.
- Fernald, F., 1984. Analysis of atmospheric lidar observation: some comments. *Applied Optics* 23, 652–653.
- Haywood, J. and Boucher, O., 2000. Estimates of the direct and indirect radiative forcing due to tropospheric aerosols: A review. *Reviews of Geophysics*, 38:513–543.
- Klett, J. D., 1981. Stable analytical inversion solution for processing lidar returns. *Applied Optics* 20, 211–220.
- Mishchenko, M. I., and Sassen, K., 1998. Depolarization of lidar returns by small ice crystals: An application to contrails. *Geophysical Research Letters* 25, 309–312.
- Sakai, T., Shibata, T., Iwasaka, Y., Nagai, T., Nakazato, M., Matsumura, T., Ichiki, A., Kim, Y.-S., Tamura, K., Troshkin, D., Hamdi, S., 2002. Case study of Raman lidar measurements of Asian dust events in 2000 and 2001 at Nagoya and Tsukuba, Japan. *Atmospheric Environment* 36, 5479–5489.
- Takamura, T., Sasano, Y., Hayasaka, T., 1994. Tropospheric aerosol optical properties derived from lidar, sun photometer, and optical particle counter measurements. *Applied Optics* 33, 7132–7140.

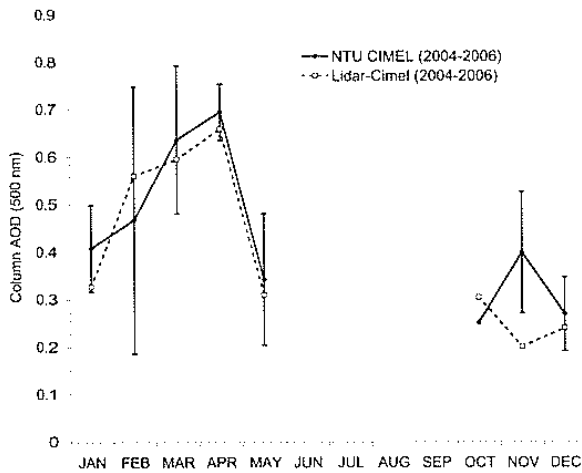


Figure 1. The monthly average values of aerosol optical thickness for coincided lidar and sun photometer measurements (dashed line) and whole set (solid line) of sun photometer during Feb. 2004 to Jan. 2006.

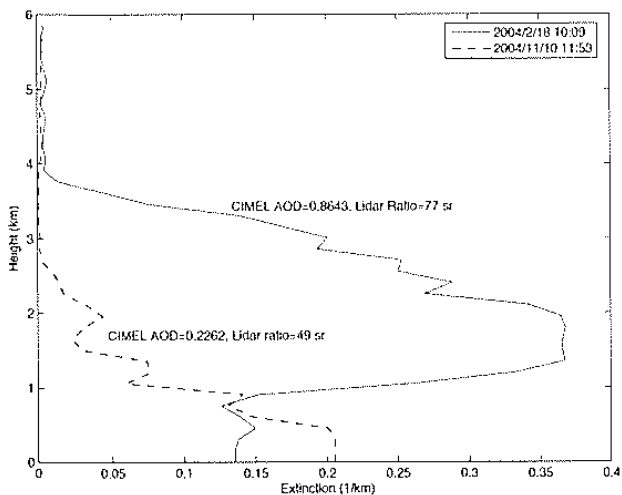


Figure 2.

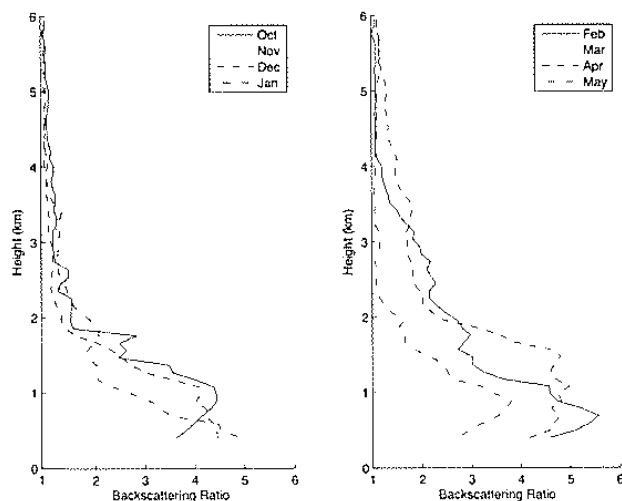


Figure 3. Monthly averaged vertical distribution of aerosol backscattering ratios measured by lidar at winter (Oct-Jan) and spring (Feb-May).

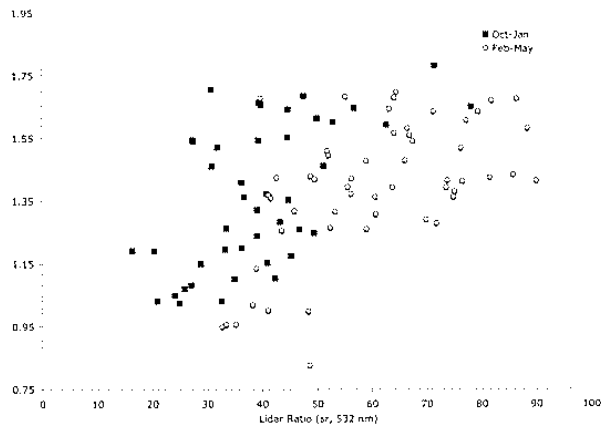


Figure 4. Scatter diagram of CIMEL angstrom exponent versus lidar ratio for the winter and the spring periods.

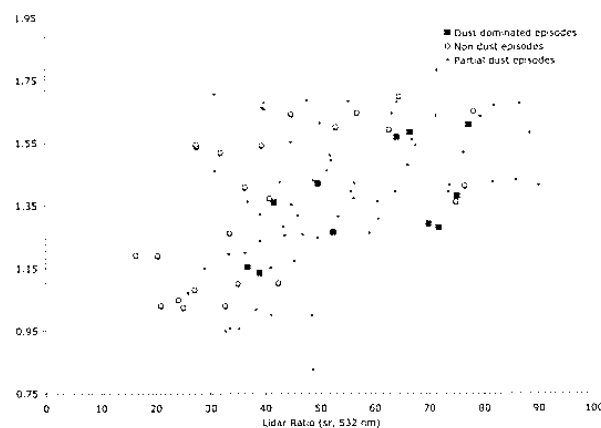


Figure 5. Same as Figure 2 but categorized by AOD fraction of Asian dust.

Table 1. Monthly average values of AOD and Angstrom exponent measured by sunphotometer. Lidar ratios were derived from combined sunphotometer and lidar measurements.

	JAN	FEB	MAR	APR	MAY	OCT	NOV	DEC
AOD	0.3266	0.5601	0.595	0.6588	0.3094	0.3037	0.1998	0.2391
Angstrom exponent	1.5005	1.257	1.505	1.242	1.298	1.222	1.542	1.3035
Lidar ratio (sr)	43	53	59	56	68	38	47	33
Fraction of AOD contributed by aerosol above 1.5 km	21%	42%	38%	31%	10%	11%	13%	7%